

Densely-Grafted and Double-Grafted PEO Brushes via ATRP. A Route to Soft Elastomers

Dorota Neugebauer,^{†,‡} Ying Zhang,^{‡,§} Tadeusz Pakula,[‡] Sergei S. Sheiko,[§] and Krzysztof Matyjaszewski^{*,†}

Center for Macromolecular Engineering, Department of Chemistry, Carnegie Mellon University, 4400 Fifth Avenue, Pittsburgh, Pennsylvania 15213; Max-Planck-Institut für Polymer Research, P.O. Box 3148, D-55021 Mainz, Germany; and Department of Chemistry, University of North Carolina at Chapel Hill, Chapel Hill, North Carolina 27599-3290

Received April 24, 2003; Revised Manuscript Received June 28, 2003

ABSTRACT: Two macromonomers containing ethylene oxide (EO) segments with different degrees of polymerization ($DP_{PEO} = 5$ and 23), capped by a methoxy and a methacrylate group (PEOMA), were polymerized by atom transfer radical polymerization (ATRP) in organic solvents. In addition to the direct preparation of densely grafted brush copolymers by “grafting through” the macromonomers, the lower molecular weight PEOMA ($MW_{av} = 300$ g/mol, $DP_{PEO} = 5$) was also employed in a “grafting from” reaction using a well-defined multifunctional macroinitiator poly(2-(2-bromopropionyloxy)ethyl methacrylate) (PBPEM, $M_{n,app} = 82 \times 10^3$ g/mol, $M_w/M_n = 1.16$, degree of polymerization of backbone $DP_b = 428$). This procedure allowed the preparation of densely double-grafted brush copolymers with various degrees of polymerization of the side chains ($DP_{sc} = 12$ –43). Attempts to prepare double-grafted brushes with $DP_{sc} > 50$ or to use a macromonomer with a longer PEO chain ($MW_{av} = 1100$ g/mol, $DP_{PEO} = 23$) in the “grafting from” reaction resulted in formation of a cross-linked gel. Both the cross-linked mono- and double-grafted brush copolymers are examples of a new class of elastomeric materials with soft rubbery properties ($G \sim 10^4$ Pa).

Introduction

Molecular brush copolymers are regularly branched macromolecules which, due to their specific architecture, assume a well-defined shape with a characteristic intramolecular density distribution. They usually consist of a linear backbone with a high grafting density of side chains (usually one side chain per repeat unit of the backbone). The backbone length, grafting density, and side chain lengths determine the total molar mass and influence the properties of materials consisting of such macromolecules.

The “grafting through” method was adapted to atom transfer radical polymerization (ATRP),^{1–3} allowing preparation of numerous graft copolymers by homopolymerization of poly(vinyl ether) macromonomers⁴ or copolymerization of a macromonomer (MM) with a low molecular weight comonomer (e.g., polystyrene–MM/*N*-vinylpyrrolidinone,⁵ poly(methyl methacrylate)–MM,⁶ or polyethylene–MM⁷ with *n*-butyl acrylate, poly(dimethylsiloxane)–MM,⁸ or polylactide–MM⁹ with methyl methacrylate). Macromonomers with hydrophilic poly(ethylene oxide) (PEO) segments have been used to prepare biocompatible materials which find application in aqueous-based systems.¹⁰ Up to now, only one poly(ethylene glycol) methyl ether with methacrylate group (PEOMA, $MW_{av} = 475$ g/mol) has been polymerized by ATRP, in aqueous media under mild conditions.^{11–14} The

procedure involved a Cu(I)/bpy catalyst system which led to 95% macromonomer conversion within 0.5 h at room temperature.¹¹ However, although the ATRP reaction was well-controlled, leading to polymers with low polydispersity ($M_w/M_n < 1.2$), the polymers prepared had a low degree of polymerization of the backbone ($DP_b = 10$ –40).¹²

ATRP was also employed for “grafting from” a backbone macroinitiator, resulting in the preparation of well-defined densely-grafted copolymers. The controlled synthesis of brush copolymers, or bottle brushes, was described for styrene (Sty)^{15,16} and several (meth)acrylate monomers including methyl (MA),¹⁷ *n*-butyl (*n*BA),^{15,16} *tert*-butyl acrylate (*t*BA),^{17,18} *n*-butyl (*n*BMA),¹⁹ and methyl methacrylate (MMA).¹⁹ This approach resulted in the preparation of bottle brush polymers with homopolymer or block copolymer side chains forming a cylindrical core–shell structure.¹⁶ In all cases the degree of polymerization of the macroinitiator was around 400. *n*BA was also grafted from a high molecular weight backbone, with $DP_b \sim 4000$,²⁰ and was grafted from a gradient copolymer of 2-(2-bromopropionyloxy)ethyl (BPPEM) and methyl methacrylate.²¹ “Grafting from” multifunctional, three- and four-armed macroinitiators was successful, yielding densely-grafted star brushes.²²

Here, we report a “grafting through” ATRP of PEOMA macromonomers, $DP_{PEO} = 5$ or 23, in organic solvents forming molecular brushes with different degrees of polymerization, DP_b . The “grafting from” reaction using both PEO macromonomers was conducted from a well-defined macroinitiator PBPEM^{15,16} ($DP_b = 334$ and 428). This procedure resulted in a new class of densely-grafted PEO copolymers, which can be considered as double-grafted brush copolymers, since each monomer unit in each of the grafts contains a PEO chain.²³

[†] Carnegie Mellon University.

[‡] Max-Planck-Institut für Polymer Research.

[§] University of North Carolina at Chapel Hill.

[‡] Permanent address: Centre of Polymer Chemistry, Polish Academy of Sciences, 34, Maria Skłodowska-Curie Str., 41-819 Zabrze, Poland.

[#] Permanent address: State Key Laboratory of Polymer Physics and Chemistry, Changchun Institute of Applied Chemistry (CAS), Changchun, China.

* Corresponding author. E-mail: km3b@andrew.cmu.edu.

Molecular brushes with very long backbones and densely-grafted PnBA side chains have an ultralow modulus plateau in the soft gel range.²⁴ When they were transformed to a network by chemical cross-linking, the material became a supersoft rubber. These unusual mechanical properties were observed for the first time in bulk polymeric brushes because the molecular network of the backbone was diluted by the short side chains. The side chains do not entangle and are covalently attached to the matrix, providing stability against evaporation or deformation, while preventing the networks from collapsing. Mechanical studies of cross-linked, mono- and double-grafted brushes indicated that they behave as soft elastomers with low values of shear modulus, G' , in the range 10^4 Pa.

Experimental Section

Materials. 2-(Trimethylsilyloxy)ethyl methacrylate (HEMA-TMS, 97.4% (GC)) was prepared as described in the Supporting Information for ref 15. Poly(ethylene glycol) methyl ether methacrylates, $\text{H}_2\text{C}=\text{C}(\text{CH}_3)\text{COO}-(\text{CH}_2\text{CH}_2\text{O})_n\text{CH}_3$ (PEOMA, $\text{MW}_{\text{av}} = 300$ g/mol, $\text{DP}_{\text{PEO}} = 5$; $\text{MW}_{\text{av}} = 1100$ g/mol, $\text{DP}_{\text{PEO}} = 23$), were obtained from Aldrich. Antioxidant inhibitors MEHQ and BHT were removed from monomers by passing through an alumina column. PEOMA with $\text{DP}_{\text{PEO}} = 23$, which is a solid at room temperature, was dissolved in THF; after removing the inhibitor, the solvent was evaporated, and the macromonomer was dried under vacuum to a constant mass. Copper(I) bromide (CuBr, Aldrich, 98%) and copper(I) chloride (CuCl, Acros, 95%) were purified by stirring with glacial acetic acid (Fisher Scientific), followed by filtration and washing the solid three times with ethanol and twice with diethyl ether. The solid was dried under vacuum (1×10^{-2} mbar) for 2 days. Copper(II) bromide (CuBr₂, Acros, 99+%) and copper(II) chloride (CuCl₂, Aldrich, 99.99%) were used as received. *p*-Toluenesulfonyl chloride (TosCl, Aldrich, 99+%) and 2,2'-azobis(isobutyronitrile) (AIBN, Aldrich, 98%) were recrystallized from hexane and ethanol, respectively, and then filtered and dried.

4,4'-Di(5-nonyl)-2,2'-bipyridine (dNbpy),²⁵ tris(2-ethylhexyl acrylate aminoethyl)amine (EHA₆TREN),²⁶ and cumyl dithiobenzoate (CDB)²⁷ were prepared as previously described. *N,N,N',N',N'*-Pentamethyldiethylenetriamine (PMDETA, Aldrich, 99%), ethyl 2-bromoisobutyrate (EtBrIBu, Aldrich, 99%), and all other solvents and internal standards were used without purification.

Characterization. Gel permeation chromatography (GPC) measurements were conducted in THF at 30 °C using a Waters 515 liquid chromatograph pump (1 mL/min) and four Polymer Standards Service columns (guard, 10^5 Å, 10^4 Å, 10^3 Å) in series with three detection systems: a differential refractometer (Waters model 410), multiangle laser light scattering (MALLS) detector (DAWN model F), and a differential viscometer (Viscotek model H502). The molecular weights of the copolymers were determined on the basis of the low polydispersity index of linear poly(methyl methacrylate) (PMMA) standards using toluene as an internal standard. The refractive index increment dn/dc was determined with an Otsuka Photol RM-102 differential refractometer.

Elemental analysis (EA) of C, H, O, and Br contents in the brush polymers was performed by Midwest Microlab (Indianapolis, IN). The degree of polymerization of the side chains based on elemental analysis ($\text{DP}_{\text{sc(EA)}}$) was calculated in the following way:

$$\text{DP}_{\text{sc(EA)}} = \frac{M_{\text{RU(EA)}} - M_{\text{BP(EM)}}}{M_{\text{PEOMA}}}; \quad M_{\text{RU(EA)}} = \frac{M_{\text{Br}} \times 100\%}{\% \text{ Br}_{\text{(EA)}}}$$

where $M_{\text{RU(EA)}}$ is the molecular weight of one repeat unit of the backbone calculated from EA, $M_{\text{BP(EM)}} = 264$ g/mol, $M_{\text{PEOMA}} = 300$ g/mol, $M_{\text{Br}} = 80$ g/mol, and $\% \text{ Br}_{\text{(EA)}}$ is the value of bromine content in the brush polymer as determined by EA.

Atomic force microscopy (AFM) images were recorded with a Nanoscope IIIa instrument (Digital Instruments) operating in the tapping mode. The measurements were performed at ambient conditions (in air, 56% relative humidity, 27 °C) using Si cantilevers with a spring constant of ca. 50 N/m, a tip radius of 8 nm, and a resonance frequency of about 300 kHz. The set-point amplitude ratio was varied in a broad range from 0.4 to 0.9 to attain clear resolution of the side chains. While the side chains were resolved at lower ratios, height profiles of adsorbed molecules were measured at higher values of the amplitude ratio to minimize tip indentation. The samples for tapping mode AFM measurements were prepared by spin-casting dilute solutions of brush molecules in chloroform at 2000 rpm.

Langmuir–Blodgett films (LB) were prepared at ambient conditions using a rectangular trough (KSV-5000) filled with double-distilled water (Milli-Q plus 185). After a 200 μL portion of a dilute solution of brushes in chloroform ($c = 1$ mg/mL) was deposited on the water surface, compression at a speed of 35 cm^2/min was initiated at a 30 min delay, so as to allow even spreading of brush molecules. The surface pressure was measured at 21 °C using a barrier/pressure transducer with a precision of 0.3 mN/m. Dense monolayers were transferred onto a mica substrate for AFM measurements. During the film transfer, the pressure was maintained constant.

Wide-angle X-ray diffraction (WAXS) and small-angle X-ray scattering (SAXS) were used to characterize the structure of the bulk materials. In both cases, the X-ray source was the $\text{CuK}\alpha$ radiation ($\lambda = 0.154$ nm) with a pinhole collimation, and 2D position-sensitive detectors (Bruker) were used. Measurements were performed at various temperatures.

The recorded scattered intensity distributions were integrated over the azimuthal angle and are presented as functions of the scattering vector ($s = 2 \sin \theta/\lambda$, where θ is the scattering angle).

Dynamic mechanical analysis (DMA) was performed using a mechanical spectrometer (RMS 800, Rheometric Scientific). Frequency dependencies of the complex shear modulus at a reference temperature (master curves) were determined from frequency sweeps measured with a small-amplitude, sinusoidal deformation at various temperatures under a dry nitrogen atmosphere. Temperature dependencies at a constant deformation rate were measured independently.

Differential scanning calorimetry (DSC) was performed with a Mettler 30 calorimeter to determine the glass transition temperatures. Heating and cooling runs were performed at a rate of 10 °C/min.

Synthesis. Polymerization of PEOMA by "Grafting Through". PEO macromonomer, ligand (with the exception of EHA₆TREN, which was added after degassing), solvent, CuBr₂ (if used in the reaction), and CuBr were added to a Schlenk flask and degassed by three freeze–pump–thaw cycles. After stirring the mixture at room temperature for 1 h the initiator, EtBrIBu, was added to start the reaction. After a predetermined time, the polymerization was stopped by opening the flask and exposing the catalyst to air. The reaction mixture was then diluted with methylene chloride and passed through activated (neutral) alumina to remove the copper complex. The remaining unreacted PEOMA macromonomer was removed by ultrafiltration in MeOH/THF (50/50 vol %) solution, and the pure brush polymer was dried under vacuum to a constant mass.

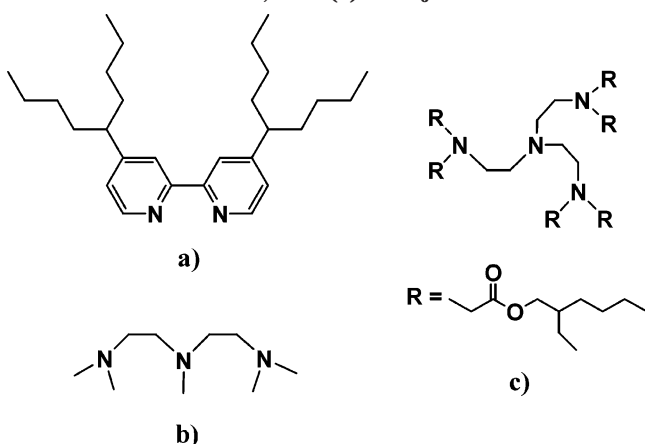
In the case of the RAFT experiment, PEOMA (2.02 g, 1.84 mmol), CDB (0.002 g, 0.007 mmol), and anisole (1.5 mL) were combined in a Schlenk flask and degassed by three freeze–pump–thaw cycles. The initiator, AIBN (0.0002 g, 0.0015 mmol) dissolved in anisole (0.5 mL), was purged with nitrogen for 10 min at 0 °C before being added to the flask. Polymerization was performed at 90 °C.

Polymerization of HEMA–TMS ($\text{DP}_n = 400$). TosCl (0.009 g, 0.05 mmol), HEMA–TMS (1 mL), and anisole (0.54 mL, 10 vol %) were combined in a 10 mL round-bottomed flask, and nitrogen was bubbled through the solution for 10 min at 0 °C. dNbpy (0.031 g, 0.075 mmol) and the rest of the monomer

Table 2. Results of Polymerization of PEOMA ($M_{w,av} = 1100$ g/mol) by "Grafting Through"^a

no.	ligand	solvent	mon/solv	temp (°C)	time (h)	conv (%) (GPC)	DP _b (GPC)	$M_{n,th}$	$M_{n,app}$ (GPC)	PDI
IIA	dNbpy	THF	1/1	60	5.5	80.7	202	222 000	102 500	2.37
IIB^b	dNbpy	THF	1/1	60	20	49.6	124	136 400	33 200	1.16
IIC	dNbpy	THF	1/2	60	5	31.6	79	86 800	30 200	1.16
IID	dNbpy	THF	1/3	60	7	17.4	43	47 900	24 200	1.13
IIE	dNbpy	toluene	1/1	60	24	47.7	119	131 300	30 200	1.15
IIF	dNbpy	anisole	1/1	80	17	23.6	59	64 900	27 800	1.16
IIG	dNbpy	MEK	1/1	80	4.5	94.0	235	258 500	54 000	2.59
IIH^{b,c}	PMDETA	anisole	1/1	90	54	89.4	223	245 300	79 900	1.96
IIJ^c	EHA ₆ TREN	anisole	1/1	60	45	81.8	204	224 400	73 600	1.47
IIK^d		anisole	1/1	60	2			gel		

^a Conditions: [PEOMA]₀: [EtBriBu]₀: [CuBr]₀: [L]₀ = 250:1:1.5:3. ^b CuBr₂ 5% vs CuBr. ^c [EtBriBu]₀: [CuBr]₀: [L]₀ = 1:2:2. ^d [AIBN]₀: [CDB]₀ (RAFT Agent) = 0.2:1.

Scheme 2. Structure of Ligands: (a) dNbpy, (b) PMDETA, and (c) EHA₆TREN

ing graft copolymer (**IIH**) has a backbone length close to that obtained with dNbpy (**IIA**, $DP_b > 200$) but had a higher polydispersity index ($M_w/M_n \sim 2$). With the PMDETA ligand, the molecular weight distribution was also broader throughout the reaction, indicating that while the catalyst rapidly activated the polymerization, the deactivation was slow in this viscous system, and many monomer units were added during each activation cycle (Figure 2).

When EHA₆TREN (Scheme 2c) ligand was used with a lower polymerization temperature ($T = 60$ °C), the rate of reaction was slower, and the reaction was better controlled, leading to a polymer (**IIJ**) with a moderately low polydispersity index ($M_w/M_n = 1.47$) and a high degree of polymerization ($DP_b = 204$). Monomodal GPC traces were obtained for the polymerization of this high molecular weight PEO macromonomer, as presented in Figure 3.

In one case, PEOMA was polymerized using reversible addition–fragmentation chain transfer (RAFT)²⁷ with AIBN as the initiator and CDB as the RAFT agent, but the reaction was faster and gel formation was observed after only 2 h (**IIK**).

Synthesis of P(BPEM-graft-PEOMA). The "grafting from" reaction was accomplished using a well-defined macroinitiator, PBPEM, prepared as previously described through ATRP of HEMA–TMS. The TMS groups were subsequently transformed to 2-bromopropionyloxy groups by esterification (Scheme 3a).^{15,16}

Multifunctional macroinitiators (**MIA**: $M_{n,app} = 82 \times 10^3$ g/mol, $M_w/M_n = 1.16$, $DP_b = 428$; **MIB**: $M_{n,app} = 64 \times 10^3$ g/mol, $M_w/M_n = 1.32$, $DP_b = 334$) were used for ATRP of a PEOMA ($M_{av} = 300$ g/mol) macromonomer yielding densely grafted brush copolymers (Scheme 3b),

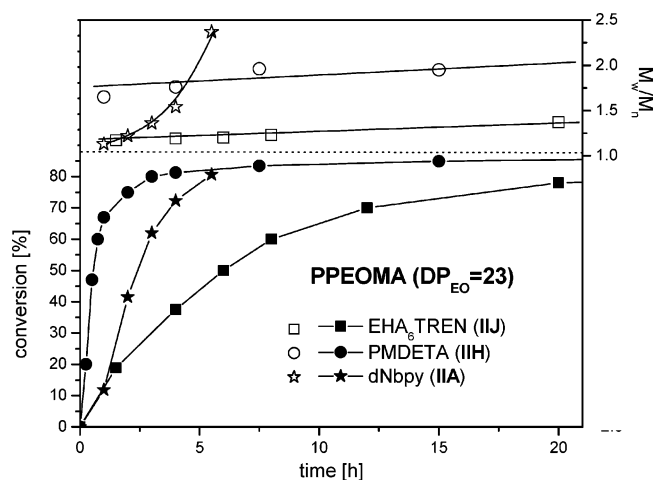


Figure 2. Conversion (left) and polydispersity (right) vs time curves for polymerization of PEOMA in the presence of various ligands. Polymerization conditions: (**IIA**) [PEOMA]₀: [EtBriBu]₀: [CuBr]₀: [dNbpy]₀ = 250:1:1.5:3; PEOMA/THF = 1/1 w/v; $T = 60$ °C; (**IIH**) [PEOMA]₀: [EtBriBu]₀: [CuBr]₀: [PMDETA]₀ = 250:1:2:2; PEOMA/anisole = 1/1 w/v; $T = 90$ °C; (**IIJ**) [PEOMA]₀: [EtBriBu]₀: [CuBr]₀: [EHA₆TREN]₀ = 250:1:2:2; PEOMA/anisole = 1/1 w/v; $T = 60$ °C.

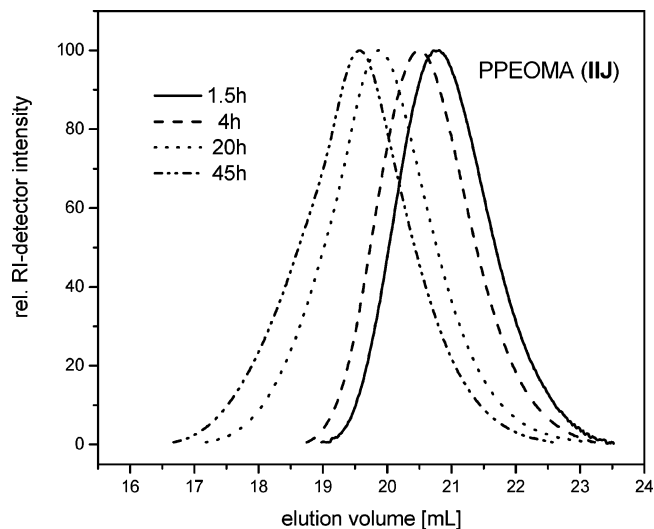
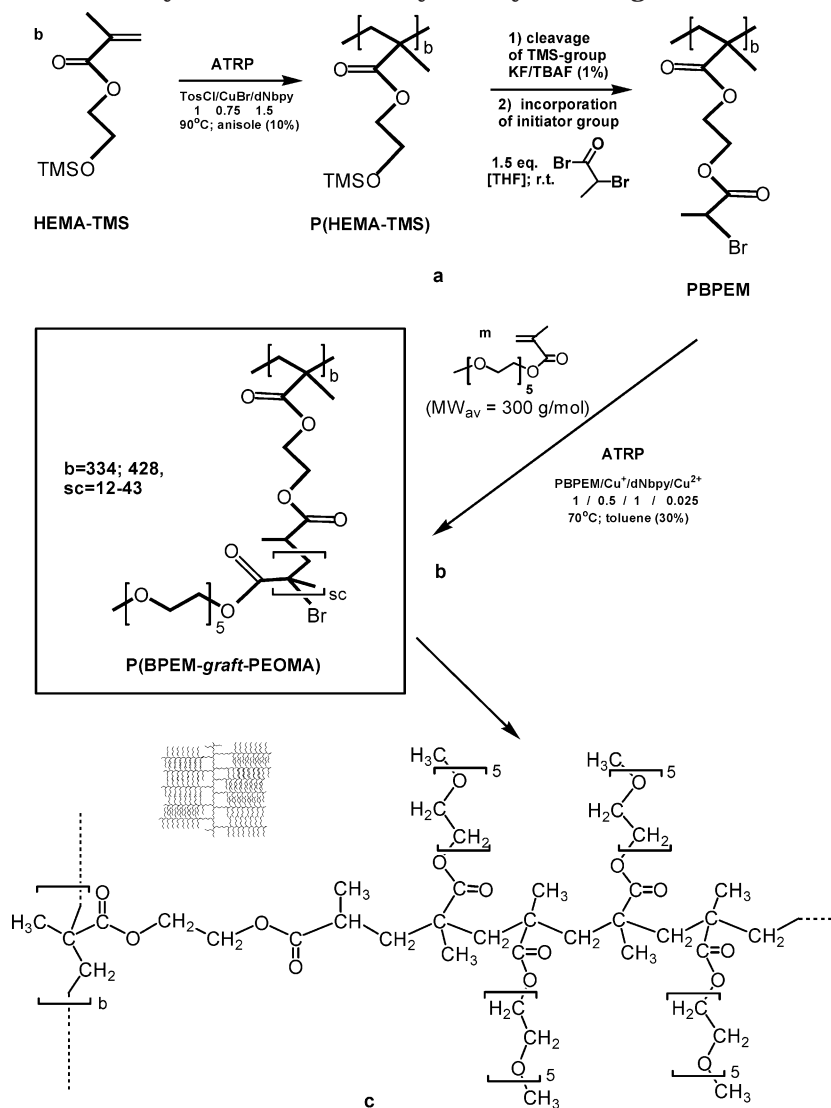


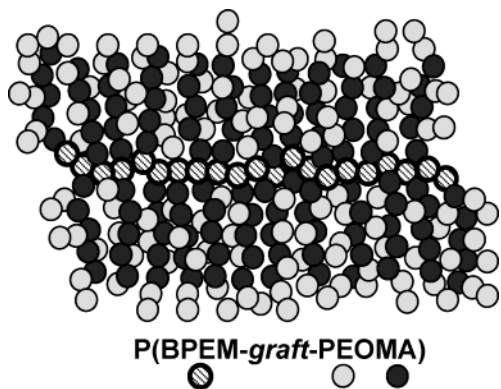
Figure 3. GPC traces of PPEOMA ($M_{w,av} = 1100$ g/mol) (**IIJ**). Polymerization conditions: [PEOMA]₀: [EtBriBu]₀: [CuBr]₀: [EHA₆TREN]₀ = 250:1:2:2; PEOMA/anisole = 1/1 w/v; $T = 60$ °C.

where each polymethacrylate side chain unit ($DP_{sc} = 12-43$) contains a short hydrophilic PEO chain ($DP_{PEO} = 5$), as presented in Scheme 3c. The resulting structure can be considered to be a double-grafted brush copoly-

Scheme 3. Synthesis of Brush Polymers by "Grafting From" PBPEM



Scheme 4. Double-Grafted Brush Copolymer



mer which has a very high density of grafted chains (Scheme 4).

The "grafting from" reaction performed in the presence of CuCl/dNbpy and 25% of deactivator CuCl₂ yielded grafted copolymer (**IIIA**) with shorter side chains within 5 h. After 10 h, the same reaction gave cross-linked product (**IIIB**). Replacing the CuCl by CuBr provides a more active catalyst resulting in a faster reaction, yielding brush polymers (**IIIC–F**) with a range of degree of polymerization, DP_{sc} = 19–43, after different reaction times. The results presented in Table 3 can

be divided into two groups. The copolymers (**IIIA** and **IIIC**) with degree of polymerization up to DP_{sc} = 19 had low polydispersity indices ($M_w/M_n = 1.2–1.3$). However, when the polymerization was continued for a longer time to obtain brushes with higher DP_{sc}, the polydispersity index increased to $M_w/M_n = 1.7$ (**IIID,E**), even though the GPC traces of the samples were still monomodal (Figure 4). In the case of brush (**IIIF**), which had the longest side chains (DP_{sc} = 43), some termination reactions also occurred which can be deduced from tailing in the GPC traces and trimodality of the molecular weight distribution, indicating brush–brush coupling. The degree of polymerizations determined by gravimetry, GC, and EA were in good agreement. When the polymerization was conducted for a longer time, a gel was formed (**IIIG**). Brush copolymer (**IIIH**) was prepared by grafting from a shorter macroinitiator with a DP_b = 334 (**MI**). The length of side chains PPEOMA increased with reaction time, and the results are presented in Table 3.

An attempt to carry out graft copolymerization of a PEOMA macromonomer, with a longer PEO chain (DP_{PEO} = 23, MW_{av} = 1100 g/mol), from the same macroinitiator resulted in formation of a cross-linked product within 1 h (Table 4). The gelation could originate from either termination or transfer reactions.

Table 3. Results of Polymerization of PEOMA ($M_{w,av} = 300$ g/mol) by "Grafting From" PBPEM^a

no.	time (h)	conv [%] (GPC)	$M_{n,th} \times 10^{-3}$	$M_{n,app} \times 10^{-3}$ (GPC)	M_w/M_n (GPC)	DP _{sc} (GPC)	DP _{sc} (grav)	DP _{sc} (EA)
MIA	0		113	82	1.16	428 ^c		
IIIA ^b	5	3.1	1553	431	1.21	12		
IIIB ^b	10							
IIIC	2	4.9	2393	700	1.28	19		
IIID	2.5	6.2	3000	904	1.66	25	25	23
IIIE	3	7.5	3713	1492	1.70	30	36	31
IIIF	6	9.7	4793	1671	1.75	39	43	38
IIIG	7							
MIB	0		88	64	1.32	334 ^c		
	1	0.6	288	119	1.17	2		
	2	1.0	489	180	1.15	4		
	5	3.3	1391	482	1.31	13		
	7	4.9	2092	638	1.43	20		
IIIH	8	6.5	2693	804	1.55	26	29	

^a Conditions: [PEOMA]₀: [PBPEM]₀: [CuBr]₀: [dNbpy]₀: [CuBr₂]₀ = 400:1:0.5:1:0.025; toluene 30 vol %; $T = 70$ °C. ^b [CuCl]₀: [CuCl₂]₀ = 0.5:0.125. ^c DP_b.

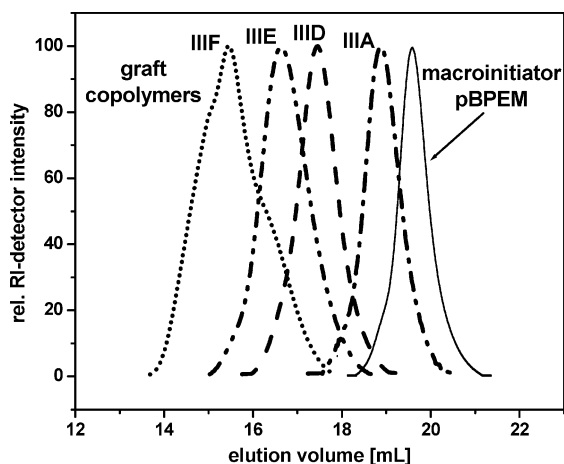


Figure 4. GPC traces of P(BPEM-*graft*-PEOMA). Polymerization conditions: (IIIA) [PEOMA]₀: [PBPEM]₀: [CuCl]₀: [dNbpy]₀: [CuCl₂]₀ = 400:1:0.5:1:0.125; PEOMA/toluene = 1/0.3 w/v; $T = 70$ °C; (IIID–F) [PEOMA]₀: [PBPEM]₀: [CuBr]₀: [dNbpy]₀: [CuBr₂]₀ = 400:1:0.5:1:0.025; PEOMA/toluene = 1/0.3 w/v; $T = 70$ °C.

Table 4. Cross-Linked Products of PEOMA ($M_{w,av} = 1100$ g/mol) Polymerization by "Grafting From" PBPEM (MIA) Macroinitiator^a

no.	[PEOMA] ₀ : [PBPEM] ₀ : [CuBr] ₀ : [dNbpy] ₀ : [CuBr ₂] ₀ (solvent)	time (h)
IVA	50:1:1:2:– (MEK 55%)	1
IVB	25:1:0.5:1:0.025 (MEK 85%)	7
IVC	10:1:0.5:1:– (THF 70%)	2

^a PBPEM (MIA): $M_{n,app} = 82$ 000; $M_w/M_n = 1.16$; DP_b = 428; $T = 50$ °C.

Atomic Force Microscopy (AFM). Figure 5 shows height images of the double-grafted PEO brush (IIIH). The higher resolution image in Figure 5a displays single molecules adsorbed on mica from a dilute solution. The molecules demonstrate the characteristic hairy morphology due to strong adsorption of the PEO side chains on the mica surface. The adsorption causes flattening of the cylindrical molecules into rectangular lamellae with a thickness of 1 nm.

The dense monolayers shown in Figure 5b were prepared by the Langmuir–Blodgett technique, as described elsewhere.²⁸ The white threads in Figure 5b correspond to the brush backbones while the area between the threads is covered by the PEO side chains. Custom software was used to analyze the length distribution of the brush molecules. The number-average contour length and the polydispersity index were de-

termined to be $L_n = 86$ nm and $L_w/L_n = 1.2$, respectively. The contour length, L_n , and the monomer length of a fully extended backbone assuming the trans zigzag conformation, l_m , allows the calculation of the degree of polymerization of the backbone, $DP_{b(AFM)} = 344$ ($DP_{b(AFM)} = L_n/l_m$, where $l_m = 0.25$ nm). The fact that the obtained value is in a good agreement with the GPC data, i.e., $DP_{b(GPC)} = 334$ (Table 3), corroborates our assumption of a fully extended backbone.

The combination of the LB and AFM techniques allows accurate measurements of the number-average molecular weight.²⁹ Using this procedure, the molecular weight was determined to be $M_{n(AFM)} = 3.2 \times 10^6$, which is close to the GPC-MALLS data, but twice as high as the molecular weight measured using universal calibration (Table 5). The average molecular weight, $M_{n(AFM)}$, was used to estimate the number-average degree of polymerization of the PPEOMA side chains from the following formula: $DP_{sc(AFM)} = (M_{n(AFM)} - M_{n,PBPEM(AFM)})/DP_{b(AFM)}/MW_{PEOMA}$, yielding a value $DP_{sc(AFM)} = 31$, which is close to the DP_{sc} determined by conversion and gravimetry (Table 3).

Complementary information about the side chain length can be extracted from the distance between molecules in the LB monolayers. Assuming a dense structure of the monolayers, an average width of 60 nm gives a number-average degree of polymerization of about 120, which is significantly higher than the DP_{sc} determined by the other techniques. This may indicate either incomplete initiation of side chains or visualization by AFM only the longest side chains with relatively high polydispersity.

Bulk Structure and Mechanical Properties. The structure and properties of the materials were characterized in order to determine the effect of the length of the PEO segments. Both the "grafted through" and the "grafted from" brushes prepared using the macromonomer with the short PEO segment ($M_{w,av} = 300$ g/mol, DP_{PEO} = 5) were amorphous, whereas the brushes from the higher molecular weight macromonomer ($M_{w,av} = 1100$ g/mol, DP_{PEO} = 23) were crystalline. Figure 6a shows typical examples of the DSC traces recorded for "grafted through" brushes from the two different macromonomers. The glass transition occurred at 212 K for the polymer with short PEO chains (IB), whereas melting and crystallization processes are indicated for the other polymer (IIK) under heating and cooling cycles, respectively. The observed melting temperature of 322 K is typical for PEO crystallites.

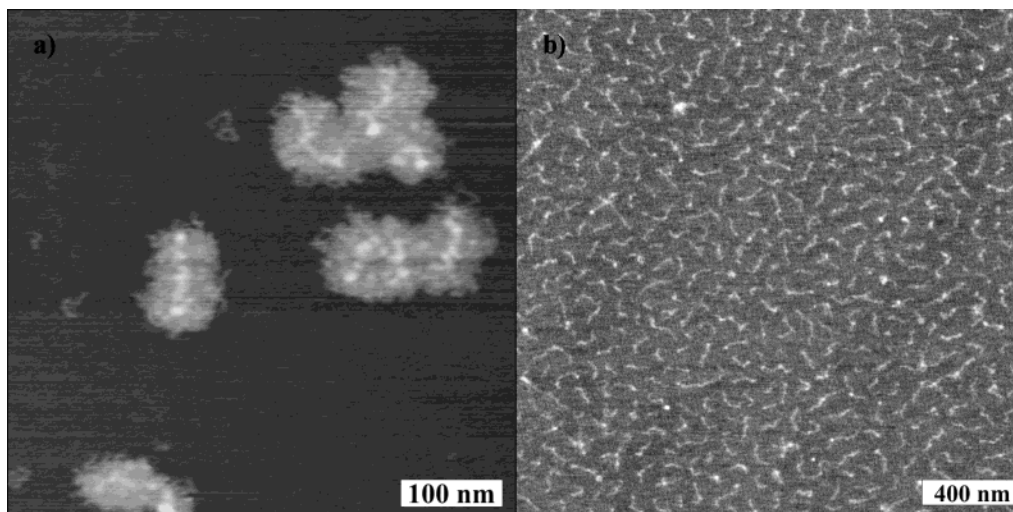


Figure 5. AFM micrographs of double-grafted brushes P(BPEM-graft-PEOMA) (**IIH**) (a) single molecules adsorbed on mica and (b) dense monolayers by LB technique.

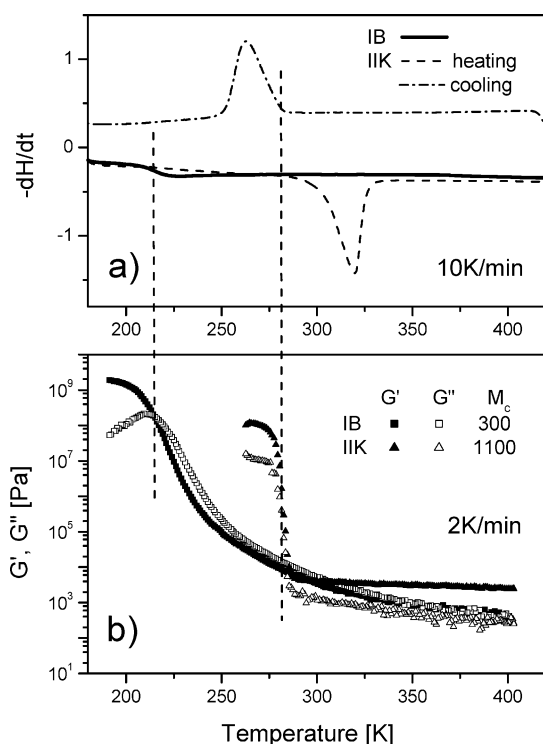


Figure 6. Thermomechanical characteristics of the hairy linear polymers obtained by “grafting through” method using two PEOMA macromonomers with different MW (**IB**: $MW_{av} = 300$ g/mol; **IIK**: $MW_{av} = 1100$ g/mol): (a) DSC traces indicating the glass transition in **IB** and melting and crystallization in **IIK**. (b) Isochronal mechanical characteristics of the two samples. The vertical dashed lines mark the glass transition in **IB** and the crystallization in **IIK** as observed by both methods.

Table 5. Molecular Weight of Brush Copolymer IIH Determined by Various Methods

GPC-MALLS		viscosity		AFM	
$M_n \times 10^{-6}$	M_w/M_n	$M_n \times 10^{-6}$	M_w/M_n	$M_n \times 10^{-6}$	M_w/M_n
2.8	1.06	1.4	1.5	3.2	1.15

Further evidence for structure-specific behavior for polymers with different length of attached PEO chains is provided by dynamic mechanical measurements (Figure 6b). The temperature dependencies of the real (G') and imaginary (G'') parts of the shear modulus show

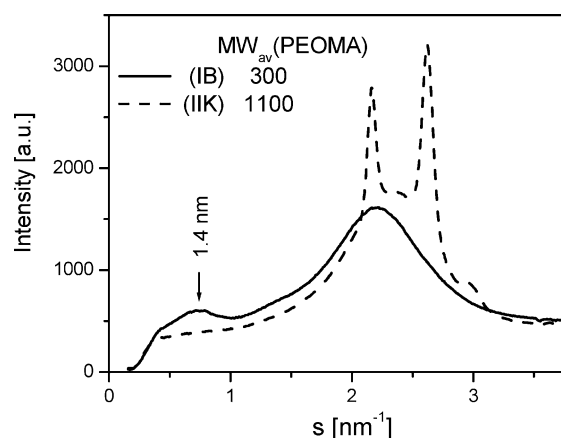


Figure 7. X-ray diffractograms of the hairy linear polymers (**IB**, **IIK**) obtained by the “grafting through” method using two macromonomers with different length of PEO segment.

that the main softening/hardening transition in the sample with short PEO chains (**IB**) is related to the temperature of transition to the glassy state (at about 220 K). In the sample (**IIK**), crystallization causes an abrupt jump in properties that takes place at about 280 K because of considerable undercooling. The modulus of the crystallized sample is lower than that of a similar polymer in the glassy state because the amorphous fraction of the material still remains soft at temperatures close to crystallization.

Structures of the two polyPEO macromonomers (**IB**, **IIK**) were examined using X-ray diffraction and small-angle X-ray scattering. The results are presented in Figure 7 and confirm the observation that the sample with shorter PEO chains (**IB**) remains amorphous whereas the other (**IIK**) is crystalline. The X-ray diffraction obtained from the polymer with shorter PEO chains displays an amorphous halo at wide angles and a broad peak in the intermediate range, indicating a correlation length of 1.4 nm. With the longer PEO chains, a typical crystalline diffraction pattern imposed on an amorphous halo is observed. In the crystalline sample, the SAXS experiments (not shown) indicated an intensity maximum (analogous to results shown in Figure 10) corresponding to distances of 15 nm, which may be attributed to periodicity in the crystalline superstructure.

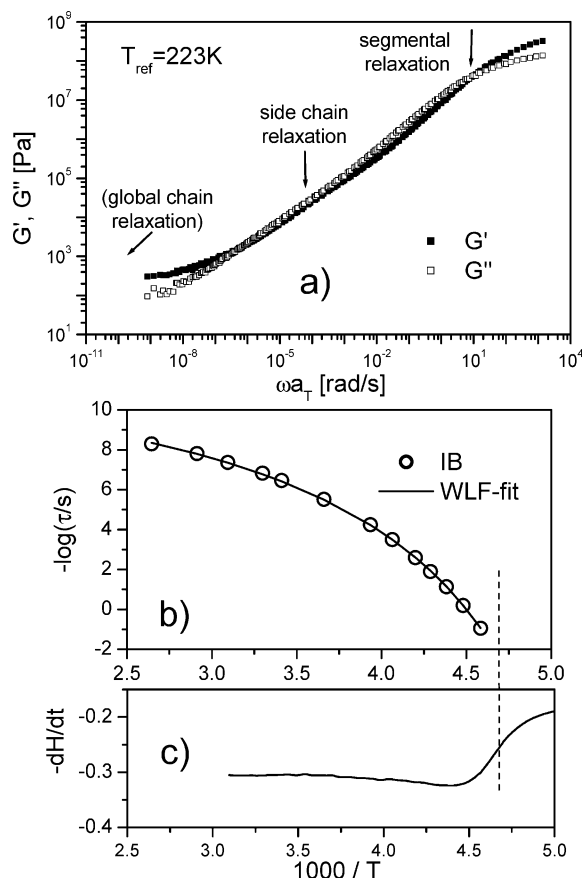


Figure 8. (a) Frequency dependencies of the real (G') and imaginary (G'') shear modulus components for a polymer **IB** obtained by the "grafting through" method, cross-linked at high conversion stages of the polymerization. (b) Temperature dependence of the segmental relaxation time and the fit of the WLF relation. (c) DSC thermogram for the same sample.

The viscoelastic spectra were determined for the amorphous samples. They characterize the mechanical behavior of the material in a broad frequency range. One such spectrum is presented in Figure 8a for polymer **IB**. In this polymer, both the segmental relaxation and the PEO side chains relaxation can be well distinguished, but global flow does not take place, at least at temperatures below 400 K. An extension of the measured frequency dependencies of G' and G'' to lower frequencies would require heating the sample to temperatures above 400 K. However, at higher temperatures the material is no longer thermomechanically simple because of additional cross-linking (samples heated to these temperatures became insoluble). In sample **IB**, instead of the expected global flow range, only a plateau in G' extending toward low frequencies is observed. This plateau indicates elastomeric properties for such polymers. The plateau modulus in this case is much lower than that seen for typical polymeric rubbers, which has to be attributed to the large fraction of the short dangling chains in the system. Such chains provide significant mobility, making the material extremely soft.

Within the range of thermomechanical simplicity, the temperature dependence of the segmental relaxation rate was determined for this sample, as shown in Figure 8b, along with the fit of the WLF relation. This relaxation slows down to 100 s at the glass transition temperature (Figure 8c), which is typical for most amorphous polymers.^{30,31}

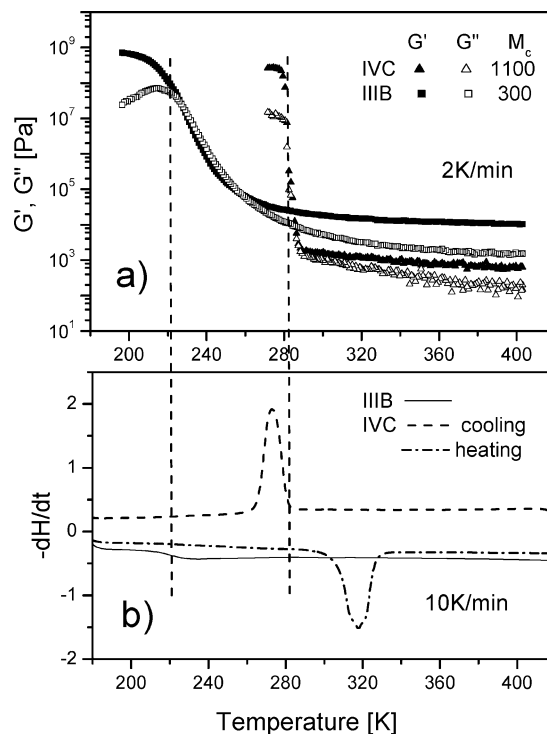


Figure 9. Thermomechanical behavior of the double-grafted brush copolymers obtained by the "grafting from" method using a macromolecular initiator and PEOMA with different MW (**IIB**: $MW_{av} = 300$ g/mol; **IVC**: $MW_{av} = 1100$ g/mol) as macromonomers: (a) Isochronal mechanical characteristics of the two samples and (b) the DSC traces indicating the glass transition in **IIB** and melting and crystallization in **IVC** both marked by the vertical dashed lines.

Grafting the PEO macromonomer from the PBPEM backbone created a double-grafted brush system. The properties of this type of material can be characterized in a manner similar to the procedure described above for mono-grafted brushes. The double-grafted brushes are either amorphous or crystalline, depending on the length of the PEO segments, as revealed by various methods.³² X-ray diffractograms analogous to those shown in Figure 6 were observed. Figure 9 compares the thermomechanical behavior of two different double-grafted brushes (**IIB** and **IVC**).

The DSC traces indicate that the double-grafted brush copolymer consisting of short PEO chains (**IIB**) is amorphous and that consisting of longer PEO chains (**IVC**) is crystalline (Figure 9b). This influences the mechanical behavior in the way illustrated in Figure 9a. In one case, the main softening of the material corresponds to the glass transition and in the other to melting or crystallization. Above these transitions the properties are remarkably dependent on the PEO chain length. It is plausible that both systems presented in Figure 9 are cross-linked and show elastic properties at high temperatures but with considerably different plateau modulus. The modulus of the polymers with longer PEO chains is smaller, which could suggest a less densely cross-linked network of backbones in this system than in the system with short PEO chains. In the double-grafted brush polymers the length of PPEOMA side chains could play an important role. However, the limited number of systems presently analyzed does not allow any unique fundamental conclusions to be drawn concerning this parameter. An example of the effect of the PPEOMA side chain length on properties and structure, when the other parameters (DP_b and

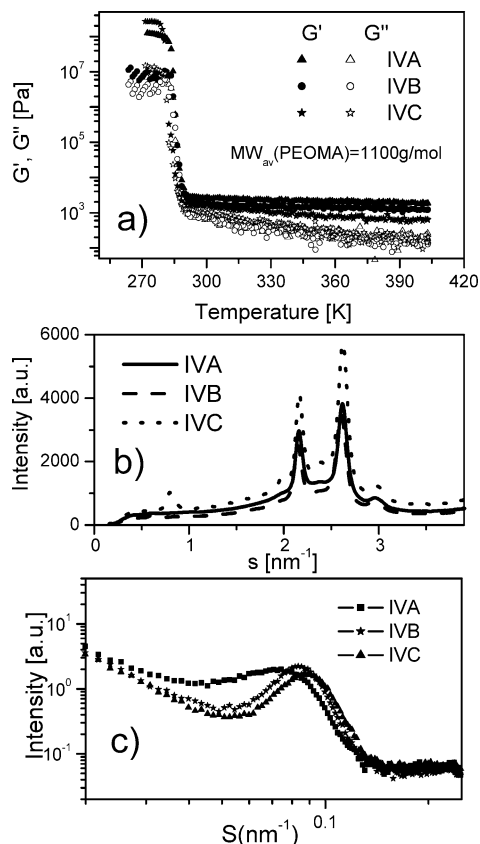


Figure 10. Effect of PPEOMA side chain length of the double-grafted brush polymers (IVA–C) obtained by the “grafting from” method using the macromolecular initiator and the PEOMA ($MW_{av} = 1100$ g/mol) as macromonomer: (a) Isochronal mechanical characteristics of the samples, (b) the wide angle diffractograms, and (c) the small-angle X-ray scattering intensity distributions vs the wave vector.

DP_{PEO}) are kept constant, is illustrated in Figure 10. As seen from both the wide- and small-angle scattering results, the systems with shorter hairy side chains have better developed crystalline structure. The modulus above the melting point increases with side chain length; nevertheless, it remains in the range characteristic for the supersoft elastomers ($G' \ll 10^4$ Pa). These observations suggest that the dynamics of the PEO chains control the systems.

In the case of the amorphous, double-grafted brushes, we were able to record the mechanical behavior characteristic for both non-cross-linked and the cross-linked structures. An example of the frequency dependencies of the real and imaginary moduli for the non-cross-linked polymer **III**E is shown in Figure 11. In this system the characteristic relaxation processes, segmental, side chain, and global relaxation (marked by the vertical dashed lines), can be distinguished. The high-frequency relaxation is the segmental motion corresponding to the glass transition of the system. The low-frequency relaxation corresponds to the polymer motion controlling macroscopic flow. The relaxation corresponding to the side chain motion is seen with a plateau of the order of 10^4 Pa. It suggests that there is a PEO chain relaxation somewhere between the segmental and the PPEOMA side chain relaxation process and that this contributes to the drop of the modulus below the conventional polymeric rubbery plateau level. The flow range is not clearly visible because of possible cross-linking taking place in the samples when the modulus

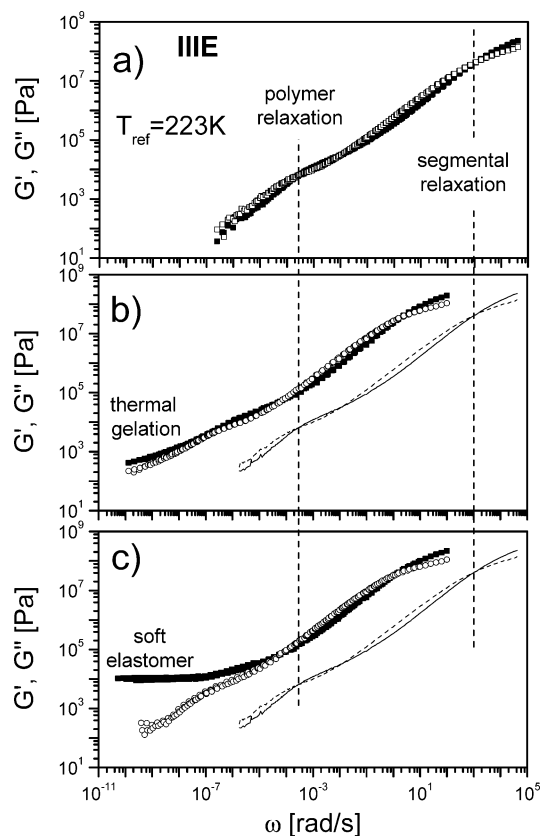


Figure 11. Frequency dependencies of the real (G') and imaginary (G'') shear modulus components for (a) non-cross-linked polymer **III**E obtained by the “grafting from” method, (b) the same polymer annealed at 100 °C, and (c) the polymer annealed at 120 °C. The annealing has been performed in a vacuum for 4 h.

is being measured at higher temperatures. This cross-linking may be indicated in greater detail by observing the effect of annealing on the viscoelastic spectra, as illustrated in parts b and c of Figure 11 for the samples annealed in the air atmosphere at temperatures 100 and 120 °C, respectively. In the annealed samples, the segmental relaxation becomes slower, and the height of the low-frequency plateau develops with annealing temperature. These samples obtained by thermally induced cross-linking also behave as soft elastomers.

A cross-linking reaction was also observed in samples polymerized to higher conversions (**III**G). An example of such a case is shown in Figure 12.

A comparison of the thermally cross-linked double-grafted brush network (**III**E, Figure 11c) with the system cross-linked during polymerization (**III**G, Figure 12) shows that the plateau moduli in both cases are similar. A modulus level in the range of 10^4 Pa indicates that the PEO chains swell and plasticize both systems. The mobility of the short non-cross-linked PEO chains makes these systems very soft in comparison to conventional networks.

Conclusions

“Grafting through” polymerization of PEOMA macromonomers under ATRP conditions yielded soluble, densely grafted brush copolymers (PPEOMA) with two different graft lengths. Use of a CuBr/dNbpy catalyst system for polymerization of a PEO macromonomer ($DP_{PEO} = 5$) allowed the successful preparation of PPEOMA with $DP_b > 400$ and $M_w/M_n = 1.18$ – 1.47 ,

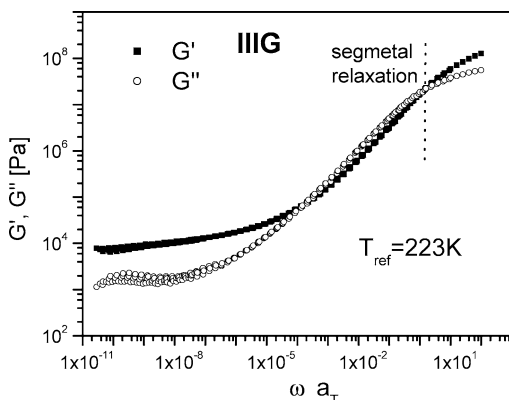


Figure 12. Frequency dependencies of the real (G') and imaginary (G'') shear modulus components for a polymers obtained by the "grafting from" method using the macromolecular initiator and the PEOMA ($M_{w,av} = 300$ g/mol) as macromonomer. The sample was cross-linked at high conversion stages of the polymerization (IIIG).

whereas the polydispersity of polymacromonomers prepared from macromonomers with a longer PEO chain ($DP_{PEO} = 23$) increased with monomer conversion, yielding graft copolymers with $DP_b = 43$ –235 and $M_w/M_n = 1.13$ –2.59.

When PMDETA was used as the ligand in the polymerization of the high MW macromonomer, a high degree of polymerization ($DP_b \sim 200$) was rapidly attained, and the polymacromonomer had a broad molecular weight distribution ($M_w/M_n = 1.96$). However, use of EHA₆TREN as the ligand decreased the polydispersity index to 1.47 for the same DP_b .

Densely double-grafted brush copolymers, with various DP_{sc} (in the range 12–43) of the main chain of the graft, have been synthesized by "grafting from" a well-defined macroinitiator PBPEM ($DP_b = 334$ and 428) using ATRP for the polymerization of the low molecular weight macromonomer PEOMA ($M_{w,av} = 300$ g/mol, $DP_{PEO} = 5$). Attempts to continue the polymerization to prepare grafts with a higher DP_{sc} (>50) or use of a PEO macromonomer with $DP_{PEO} = 23$ led to gelation of the reaction mixture. The hairy morphology of double-grafted brush copolymers was observed by AFM.

The remarkable properties seen for these materials result from the presence of a high density of nonentangled side chains grafted along the macromolecular backbone. The modulus of such systems in the rubbery range is strongly dependent on the architecture of the brushlike macromolecules. Cross-linking of either the mono- or double-grafted copolymers results in the formation of elastomers that display new properties for a bulk stable material. These properties are typical for a soft rubber ($G' \sim 10^4$ Pa).

Acknowledgment. This work was financially supported by the National Science Foundation ECS 01-03307, CRP Consortium at CMU, NATO Science Fellowships Programme (D.N.), and the program of cooperation between Chinese Academy of Sciences and the Max-Planck Society (Y.Z.).

References and Notes

- (1) Wang, J. S.; Matyjaszewski, K. *J. Am. Chem. Soc.* **1995**, *117*, 5614.
- (2) Matyjaszewski, K.; Xia, J. *Chem. Rev.* **2001**, *101*, 2921.
- (3) Kamigaito, M.; Ando, T.; Sawamoto, M. *Chem. Rev.* **2001**, *101*, 3689.
- (4) Yamada, K.; Miyazaki, M.; Ohno, K.; Fukuda, T.; Minoda, M. *Macromolecules* **1999**, *32*, 290.
- (5) Matyjaszewski, K.; Beers, K. L.; Kern, A.; Gaynor, S. G. *J. Polym. Sci., Part A: Polym. Chem.* **1998**, *36*, 823.
- (6) Roos, S. G.; Mueller, A. H. E.; Matyjaszewski, K. *Macromolecules* **1999**, *32*, 8331.
- (7) Hong, S. C.; Matyjaszewski, K.; Gottfried, A. E.; Brookhard, M. *Polym. Mater. Sci. Eng.* **2001**, *84*.
- (8) Shinoda, H.; Miller, P. J.; Matyjaszewski, K. *Macromolecules* **2001**, *34*, 3186.
- (9) Shinoda, H.; Matyjaszewski, K. *Macromolecules* **2001**, *34*, 6243.
- (10) Harris, J. M. *Poly(Ethylene Glycol) Chemistry and Biotechnical and Biomedical Applications*; Plenum Press: New York, 1972.
- (11) Wang, X. S.; Lascelles, S. F.; Jackson, R. A.; Armes, S. P. *Chem. Commun.* **1999**, 1817.
- (12) Haddleton, D. M.; Perrier, S.; Bon, S. A. F. *Macromolecules* **2000**, *33*, 8246.
- (13) Wang, X. S.; Malet, F. L. G.; Armes, S. P.; Haddleton, D. M.; Perrier, S. *Macromolecules* **2001**, *34*, 162.
- (14) Perrier, S.; Armes, S. P.; Wang, X. S.; Malet, F. L. G.; Haddleton, D. M. *J. Polym. Sci., Part A: Polym. Chem.* **2001**, *39*, 1696.
- (15) Beers, K. L.; Gaynor, S. G.; Matyjaszewski, K.; Sheiko, S. S.; Moeller, M. *Macromolecules* **1998**, *31*, 9413.
- (16) Boerner, H. G.; Beers, K. L.; Matyjaszewski, K.; Sheiko, S. S.; Moeller, M. *Macromolecules* **2001**, *34*, 4375.
- (17) Beers, K. L. Ph.D. Thesis, Pittsburgh, PA, 2000.
- (18) Cheng, G.; Boeker, A.; Zgang, M.; Krausch, G.; Mueller, A. H. E. *Macromolecules* **2001**, *34*, 6883.
- (19) Neugebauer, D.; Matyjaszewski, K.; da Silva, M.; Sheiko, S. S. *Polym. Prepr. (Am. Chem. Soc., Div. Polym. Chem.)* **2002**, *43*, 239.
- (20) Qin, S.; Boerner, H. G.; Matyjaszewski, K.; Sheiko, S. S. *Polym. Prepr. (Am. Chem. Soc., Div. Polym. Chem.)* **2002**, *43*, 237.
- (21) Boerner, H. G.; Duran, D.; Matyjaszewski, K.; da Silva, M.; Sheiko, S. S. *Macromolecules* **2002**, *35*, 3387.
- (22) Matyjaszewski, K.; Qin, S.; Boyce, J. R.; Shirvanyants, D.; Sheiko, S. S. *Macromolecules* **2003**, 1843.
- (23) Neugebauer, D.; Matyjaszewski, K. *Polym. Prepr. (Am. Chem. Soc., Div. Polym. Chem.)* **2002**, *43*, 241.
- (24) Pakula, T.; Matyjaszewski, K. *Nature Mater.*, submitted.
- (25) Matyjaszewski, K.; Patten, T. E.; Xia, J. *J. Am. Chem. Soc.* **1997**, *119*, 674.
- (26) Gromada, J.; Matyjaszewski, K. *Polym. Prepr. (Am. Chem. Soc., Div. Polym. Chem.)* **2002**, *43*, 195.
- (27) Chiefari, J.; Rizzardo, E. In *Handbook of Radical Polymerization*; Matyjaszewski, K., Davis, T. P., Eds.; John Wiley & Sons: New York, 2002; p 629.
- (28) Sheiko, S. S.; Prokhorova, S. A.; Beers, K.; Matyjaszewski, K.; Potemkin, I. I.; Khokhlov, A. R.; Möller, M. *Macromolecules* **2001**, *34*, 8354.
- (29) Sheiko, S. S.; da Silva, M.; Shirvanyants, D. G.; Larue, I.; Prokhorova, S. A.; Möller, M.; Beers, K.; Matyjaszewski, K. *J. Am. Chem. Soc.* **2003**, *125*, 6725.
- (30) Pakula, T.; Geyler, S.; Edling, T.; Boese, D. *Rheol. Acta* **1996**, *35*, 631.
- (31) Gohr, K.; Pakula, T.; Tsutsumi, K.; Schärfl, W. *Macromolecules* **1999**, *32*, 7156.
- (32) Pakula, T.; Vlassopoulos, D.; Fytas, G.; Roovers, J. *Macromolecules* **1998**, *31*, 8931.

MA0345347